Serine Catabolism by SHMT2 Is Required for Proper Mitochondrial Translation Initiation and Maintenance of Formylmethionyl-tRNAs

Published in final edited form as:

Mol Cell. 2018 February 15; 69(4): 610–621.e5. doi:10.1016/j.molcel.2018.01.024.

Serine Catabolism by SHMT2 is Required for Proper Mitochondrial Translation Initiation and Maintenance of Formylmethionyl tRNAs

Denise R. Minton[1,5], **Minwoo Nam**[1,5], **Daniel J. McLaughlin**[1,5], **Jong Shin**[1], **Erol C. Bayraktar**[2], **Samantha W. Alvarez**[1], **Vladislav O. Sviderskiy**[1], **Thales Papagiannakopoulos**[1], **David M. Sabatini**[3], **Kıvanç Birsoy**[2], and **Richard Possemato**[1,4]

[1]Department of Pathology, New York University School of Medicine, New York, New York, 10016 USA. Laura & Isaac Perlmutter Cancer Center, NYU School of Medicine, New York, NY 10016, USA

[2]Laboratory of Metabolic Regulation and Genetics, The Rockefeller University, 1230 York Avenue, New York, NY 10065, USA

[3]Whitehead Institute for Biomedical Research, Nine Cambridge Center, Cambridge, Massachusetts 02142, USA; Howard Hughes Medical Institute and Department of Biology, Massachusetts Institute of Technology, Cambridge, Massachusetts 02139, USA; The David H. Koch Institute for Integrative Cancer Research at MIT, 77 Massachusetts Avenue, Cambridge, Massachusetts 02139, USA; Department of Biology, Massachusetts Institute of Technology (MIT), Cambridge, Massachusetts 02139, USA; Broad Institute of Harvard and MIT, Seven Cambridge Center, Cambridge, Massachusetts 02142, USA

Summary

Upon glucose restriction, eukaryotic cells upregulate oxidative metabolism to maintain homeostasis. Using genetic screens, we find that the mitochondrial serine hydroxymethyltransferase (SHMT2) is required for robust mitochondrial oxygen consumption and low glucose proliferation. SHMT2 catalyzes the first step in mitochondrial one-carbon metabolism which, particularly in proliferating cells, produces tetrahydrofolate (THF)-conjugated one-carbon units used in cytoplasmic reactions despite the presence of a parallel cytoplasmic pathway. Impairing cytoplasmic one-carbon metabolism or blocking efflux of one-carbon units from

Correspondence: Richard.possemato@nyumc.org, KBirsoy@mail.rockefeller.edu.
[4]Lead Contact
[5]These authors contributed equally.

DECLARLATION OF INTERESTS

D.M.S. is a founding member of the scientific advisory board, a paid consultant, and a shareholder of Navitor Pharmaceuticals.

AUTHOR CONTRIBUTIONS

Conceptualization, R.P., K.B., and D.M.S.; Methodology, R.P. and K.B.; Investigation, K.B. and E.C.B. (CRISPR screen and analysis), M.N. and J.S. ($tRNA^{Met}$ northern blotting), T.P. (pSECB vector design and generation), D.R.M., D.J.M, M.N., R.P., V.O.S., and S.W.A. (all remaining experiments); Writing – Original Draft, D.R.M. and R.P.; Writing – Review & Editing, D.R.M, R.P., and K.B.; Funding Acquisition, Resources, and Supervision, R.P. and K.B.

mitochondria does not phenocopy SHMT2 loss, indicating that a mitochondrial THF cofactor is responsible for the observed phenotype. The enzyme MTFMT utilizes one such cofactor, 10-formyl THF, producing formylmethionyl-tRNAs, specialized initiator tRNAs necessary for proper translation of mitochondrially encoded proteins. Accordingly, SHMT2-null cells specifically fail to maintain formylmethionyl-tRNA pools and mitochondrially encoded proteins, phenotypes similar to those observed in MTFMT deficient patients. These findings provide a rationale for maintaining a compartmentalized one-carbon pathway in mitochondria.

Graphical Abstract

Using CRISPR/Cas9-based screening, Minton et al identify serine catabolic enzyme SHMT2 as differentially required in low glucose. Via SHMT2, serine contributes to mitochondrial one-carbon pools, THF-based cofactors required for carbon transfer reactions including mitochondrial initiator tRNA formylation. Therefore, SHMT2 loss impacts mitochondrial translation, depleting mitochondrially encoded proteins and decreasing respiration.

Introduction

Restriction of glucose, either by growth in glucose limited conditions or by providing alternative, slowly metabolized carbon sources such as galactose, increases the dependence of cells on genes involved in mitochondrial oxidative phosphorylation (OXPHOS) (Arroyo et al., 2016; Birsoy et al., 2014; Robinson et al., 1992). Mutation of such genes frequently underlies mitochondrial disease in human patients, such as Leigh Syndrome, and loss of mitochondrial complex expression or respiration has been observed in several aging associated diseases, such as neurodegeneration, stem cell exhaustion, and cancer (Wallace, 1999). Furthermore, growing tumors experience glucose limitation due to a combination of inadequate vasculature and excessive cell proliferation (Gullino et al., 1967; Hirayama et al., 2009). The ability of cancer cells to survive in such a metabolically challenging environment is likely to be a key adaptation in cancer, which can create novel targetable metabolic liabilities (Cantor and Sabatini, 2012; Vander Heiden and DeBerardinis, 2017). Therefore, to identify genes required for mitochondrial respiration and survival in low glucose, we previously developed a continuous flow cell culture system termed a nutrostat, enabling extended cell proliferation in glucose limiting conditions (Birsoy et al., 2014). We used this system to perform an RNAi based loss-of-function screen, resulting in the identification of multiple core subunits of OXPHOS and glucose transporters as differentially required in low glucose (Birsoy et al., 2014). Here, we extend on these findings using CRISPR/Cas9 based screening methods, and surprisingly identify the one-carbon metabolism enzyme SHMT2 as being required for proliferation a in low glucose environment.

SHMT2 catalyzes the first of a series of four reactions comprising mitochondrial one-carbon metabolism (Ducker and Rabinowitz, 2017; Stover and Schirch, 1990). The bifunctional enzymes encoded by MTHFD2/2L, as well as MTHFD1L, catalyze the remaining steps providing serine derived one-carbon units for cytoplasmic reactions requiring a tetrahydrofolate (THF)-coupled methyl donor, such as thymidine synthesis, methionine recycling, and purine synthesis. Eukaryotes maintain a parallel pathway in the cytoplasm catalyzed by enzymes encoded by SHMT1 and the trifunctional MTHFD1, revealing a high

degree of metabolic compartmentalization (Appling, 1991). Interestingly, mice lacking SHMT1 have no overt phenotype, whereas loss of MTHFD2 or MTHFD1L are embryonic lethal, leading to the conclusion that the mitochondrial SHMT2 could compensate for loss of the cytoplasmic SHMT1, and that carbon charged THF cofactors produced in the cytoplasm could not pass through the mitochondrial membrane to overcome deficits in the mitochondrial compartment (Di Pietro et al., 2002; MacFarlane et al., 2008; Momb et al., 2013). Surprisingly, enzymes of mitochondrial one-carbon metabolism are frequently silenced or poorly expressed in non-proliferative adult tissues, but become highly upregulated upon initiation of cell proliferation (Mejia and MacKenzie, 1985; Nilsson et al., 2014). These observations have led to the conclusion that one primary route of serine catabolism in proliferative cells is via harvesting of its carbon by mitochondrial one-carbon metabolism, followed by the export of these one-carbon units to the cytoplasm for use in the above mentioned reactions. Here, we describe the key role of SHMT2 and mitochondrial one carbon metabolism in supporting cellular proliferation in low glucose conditions. SHMT2 null cells exhibit defects in mitochondrial respiration and a corresponding loss of proteins translated in the mitochondria, without effects on cytoplasmic translation. Using cell-based models in which additional enzymes of one carbon metabolism have been deleted, we conclude that loss of THF-conjugated one-carbon units from the mitochondria underlie the observed SHMT2 knockout phenotype. Specifically, we find that SHMT2 deletion results in loss of the product of a tRNA formylation reaction, fMet-tRNA^{Met}, catalyzed by the enzyme MTFMT and requiring 10-formyl THF as a formyl donor. This modified tRNA is used to initiate translation specifically in mitochondria, and its loss is observed in patients with mitochondrial disease.

Results

A CRISPR/Cas9 based genetic screen identifies SHMT2 as being differentially required in low glucose conditions

In previous studies, we used RNAi based genetic screening approaches in Jurkat leukemic T cells to define a set of genes differentially required in low glucose conditions, maintained using a continuous flow cell culture system termed a nutrostat (Birsoy et al., 2014). Here, we replicated this approach using CRISPR/Cas9 based screening methods to compare the two methods and determine if additional differentially required genes would be revealed by using an approach that has the capacity to generate a complete loss of function (Figure 1A). We used an analogous sgRNA library containing 30,000 small guide RNAs (sgRNAs) targeting 2,948 metabolic enzymes and small molecule transporters (10 sgRNAs/gene) as well as 500 control sgRNAs (Birsoy et al., 2015) (Figure 1A). Metabolic enzymes were defined as enzymes which act upon small molecules (not upon macromolecules such as proteins, DNA, or RNA) and small molecule transporters were defined as proteins which permit the movement of such small molecules across plasma membranes. We infected Jurkat cells with this sgRNA library and cultured them in nutrostats set to 10 mM or 0.75 mM glucose containing RPMI media, and determined the abundance of sgRNAs in the pool at the beginning and end of the culture period by deep sequencing. For each gene, we calculated an essentiality score in these conditions based on the median performance of all 10 sgRNAs (Table S1).

Similar to the RNAi-based screen, many of the genes selectively required for proliferation in low glucose encode for subunits of the mitochondrial electron transport chain (ETC), particularly Complex I, the components of which scored significantly better than components of Complexes III, IV, or V (Figure 1B and S1). These results further support the observation that the ETC is the major pathway required for optimal proliferation in low glucose. Also identified as being differentially required in low glucose are several mitochondrially localized genes (Calvo et al., 2016) including heme biosynthetic enzyme porphobilinogen deaminase (*HMBS*), a phosphate transporter (*SLC25A3*), a zinc transporter (*SLC30A9*), malonyl CoA-acyl carrier protein transacylase (*MCAT*), Coenzyme Q prenylating enzyme decaprenyl-diphosphate synthase subunit 2 (*PDSS2*), and StAR-related lipid transfer domain protein 7 (*STARD7*). These genes are likely required for proper ETC function.

The highest non-ETC scoring gene is the mitochondrial serine hydroxymethyltransferase 2 (*SHMT2*), which catalyzes the reversible reaction of serine and tetrahydrofolate to glycine and 5,10-methylene tetrahydrofolate, directing serine derived carbon into the one-carbon pool. However, a direct role for mitochondrial one-carbon metabolism in mitochondrial ETC function has not been described. To validate the screening results, we used CRISPR/Cas9 based methods to generate two clonal Jurkat cell lines in which SHMT2 protein was undetectable (sgSHMT2_1 and 2) (Figure 1C, D). While SHMT2-null cells proliferate more slowly than parental cells in 10 mM glucose, they are particularly sensitive to culture in 1.5 mM glucose (Figure 1E). However, these phenotypes were not accompanied by an altered cell cycle profile and markers of apoptosis or DNA damage were not affected (Figure S2). Reintroduction of SHMT2 into one of the SHMT2-null cell lines by expressing an SHMT2 cDNA restored SHMT2 protein levels and significantly rescued these proliferation defects (Figure 1C–E). To determine whether loss of SHMT2 catalytic activity is required for the observed low glucose sensitivity in the SHMT2-null cell lines, we generated an SHMT2 cDNA in which a key catalytic residue (K280, (Schirch et al., 1993)) had been mutated to alanine (CD SHMT2). Unlike the wildtype enzyme, the catalytic dead SHMT2 mutant was unable to rescue the effects of SHMT2 deletion on proliferation in high or low glucose (Figure 1D, F). Therefore SHMT2 catalytic activity is required for proliferation in low glucose conditions.

SHMT2 is required for proper mitochondrial respiration and translation of mitochondrially encoded proteins

Given the clear role of the ETC in supporting cell proliferation upon glucose limitation, we considered whether SHMT2 loss could impact cellular respiration. Indeed, we observed a 69.1% reduction in the basal oxygen consumption rate of SHMT2-null Jurkat cells and a 68.9% reduction in mitochondrial ATP production compared to parent Jurkat cells (Figs. 2A–C). Culture in low glucose leads to an increase in the OCR in many cell types as cells adjust to decreased glycolytic flux by increasing mitochondrial oxidation of glucose (Birsoy et al., 2014; Crabtree, 1929). Similarly, treatment with the ETC uncoupling agent FCCP increases the rate or respiration to the maximum achievable by the cell. In both conditions, SHMT2-null cells exhibited an ability to modestly increase in their oxygen consumption rate, but only to approximately 50% of wild-type levels (Figure 2A). We also analyzed

intracellular metabolites from SHMT2-null cell lines grown in 10 mM and 1 mM glucose and noted that the levels of glycine and aspartate were decreased in the mutant cell lines under both glucose conditions (Figure 2D, S3A). Glycine is a product of the SHMT2 reaction, hence reduction in glycine levels is an expected consequence of SHMT2 loss, and has been observed upon SHMT2 knockdown by RNAi (Kim et al., 2015). Interestingly, maintenance of aspartate levels is a key function of the ETC (Birsoy et al., 2015; Sullivan et al., 2015). Thus, the loss of aspartate is consistent with the reduction of oxygen consumption observed upon SHMT2 deletion. However, deficiencies in the levels of these particular amino acids could not themselves explain the effect of SHMT2 deletion on cell proliferation, as their supplementation had no effect on this phenotype (Figure S3B).

One hypothesized advantage of the reliance of proliferative cells on mitochondrial serine catabolism is the ability of mitochondrial one-carbon metabolism to generate NADPH, which could be useful in times of high oxidative stress or for the biosynthesis of dNTPs and fatty acids (Fan et al., 2014; Ye et al., 2014). We therefore assessed whether the phenotypes observed upon SHMT2 deletion could be the result of defective oxidative stress management. However, we did not observe an increase in overall reactive oxygen species (ROS) as measured by ROS-reactive dyes, nor was anti-oxidant treatment able to recover any of the proliferative capacity lost upon SHMT2 deletion (Figure S2, S3B).

Based on the significant impairment in respiration upon SHMT2 knockout, we proceeded to assess the underlying cause of the defect. We did not observe substantial changes in mitochondrial DNA content, mass, or membrane potential in the SHMT2-null cells (Figure 2E–G), and mitochondrial RNA levels were not consistently altered, although modest changes in the abundance of individual regions was observed (Figure 2H, S3C). However, upon immunoblotting for mitochondrial proteins, we detected a significant reduction in the levels of mitochondrially encoded cytochrome c oxidase I and II (MT-COI and MT-COII) and NADH-ubiquinone oxidoreductase chain 1 (MT-ND1), but no difference in the levels of nuclear-encoded cytochrome c oxidase subunit IV (COX4) (Figure 2I). These phenotypes were rescued by the introduction of SHMT2, but not CD SHMT2 (Figure 2I, S3D). Consistent with these findings, the SHMT2-null cells have reduced synthesis of specific mtDNA-encoded proteins as assayed by [^{35}S]-cysteine and methionine labeling of mitochondrially encoded proteins (Figure 2J), similar to previous observations made in patient fibroblasts with defects in mitochondrial translation (Hinttala et al., 2015; Tucker et al., 2011). In contrast, labeling of proteins translated in the cytosol is not impacted (Figure 2J).

To determine if these defects can be observed widely across transformed cell types and species, we chose a panel of cell lines (TT esophageal cancer, MCF10DCIS.com and MCF-7 breast cancer cell lines, and a cell line, KP, derived from a Kras mutant and Tp53 loss-of-function lung cancer mouse model) and deleted SHMT2 using the sgRNAs described above, or two directed against murine Shmt2 (Figure S4). These SHMT2-null cell lines exhibited a decrease in oxygen consumption and mitochondrially encoded proteins similar to that observed in Jurkat cells, phenotypes rescued by expression of an SHMT2 cDNA (Figure S4). SHMT2 loss was also accompanied by sensitivity to glucose limitation in TT and KP, but not MCF-7 cells, which did not exhibit substantial sensitivity to glucose restriction, or in

MCF10DCIS.com cells (Figure S4). Furthermore, these observations extended to cells growing in an in vivo context, as tumors derived from SHMT2-null MCF10DCIS.com cells also exhibited selective loss of mitochondrially encoded proteins (Figure S4M). Collectively, these data demonstrate that SHMT2 is required for proper translation of mitochondrial-encoded proteins in multiple contexts.

Depletion of mitochondrial one-carbon units upon SHMT2 loss prevents proper mitochondrial translation

One-carbon metabolism takes place in both the cytoplasm and the mitochondria, with parallel reactions taking place in a highly compartmentalized manner (Figure 3A). To determine whether the observed impact on mitochondrial respiration and translation is specific to disruption of mitochondrial one-carbon metabolism, we investigated the role of the cytosolic serine hydroxymethyltransferase, SHMT1. We overexpressed an SHMT1 cDNA in SHMT2-null Jurkat cells or used CRISPR/Cas9 mediated techniques to generate two SHMT1-null Jurkat cell lines (+sgSHMT1_1 and 2), and verified SHMT1 expression by immunoblotting (Figure 3B). Over-expression of SHMT1 in SHMT2-null cells did not rescue the low glucose sensitivity or mitochondrial respiration defects, and did not affect the levels of mitochondrially translated proteins (Figure 3B–D). Similarly, SHMT1-null cells were indistinguishable from parent Jurkat cells with respect to these phenotypes (Figure 3B–D). Therefore, impairment of mitochondrial metabolism and sensitivity to low glucose are specifically the result of losing mitochondrial serine hydroxymethyltransferase activity.

To determine if the effects of deleting SHMT2 on the mitochondria are specifically due to disruption of the efflux of one-carbon units from the mitochondria, we next performed CRISPR/Cas9-mediated deletion of MTHFD1L, the final enzyme in this mitochondrial one-carbon pathway, and verified loss of MTHFD1L by immunoblotting (Figure 3E). MTHFD1L catalyzes the reversible conversion of 10-formyl THF to THF and formate, which can exit the mitochondria and contribute to the cytosolic one-carbon pool (Figure 3A). Therefore, deletion of SHMT2 or MTHFD1L will each prevent one-carbon units produced in the mitochondria from contributing to the cytoplasmic pool. In contrast, MTHFD1L-null cells should still have mitochondrial THF-conjugated one-carbon units available for reactions requiring these cofactors, whereas SHMT2-null cells should not. Interestingly, unlike SHMT2 deletion, loss of MTHFD1L did not impact mitochondrial respiration, mitochondrial protein levels, or low glucose sensitivity, and only resulted in modest effects on overall proliferation that differed between individual clones (Figure 3F–G). These results indicate that depletion of the mitochondrial one-carbon pool, and not flux of one-carbon units from the mitochondria to the cytoplasm, is responsible for the SHMT2 knockout phenotype.

Disruption of SHMT2 would be predicted to result in the depletion from the mitochondria of both its immediate product, 5,10-Me THF, as well as 10-formyl THF, the product of a downstream reaction catalyzed by the enzymes MTHFD2 and MTHFD2L (Figure 3A). To further refine which of these cofactors are most likely to be responsible for the observed phenotypes upon SHMT2 deletion, we used CRISPR/Cas9 mediated techniques to generate Jurkat cell lines in which MTHFD2, MTHFD2L, or both enzymes were deleted

(+sgMTHFD2_1 and 2 or +sgMTHFD2L_1 and 2). Loss of MTHFD2 and MTHFD2L were verified by immunoblotting (Figure 3H). MTHFD2L-null cells retained wild-type levels of oxygen consumption and mitochondrially translated proteins, whereas MTHFD2-null cells exhibited a slight reduction in these phenotypes compared to SHMT2 null cells (Figure 3H,I). Importantly, MTHFD2/2L double knockout cells exhibited a significant reduction in oxygen consumption and loss of mitochondrially encoded proteins, on the scale of that observed upon SHMT2 deletion (Figure 3H–I). These results implicate 10-formyl THF as a relevant cofactor lost in SHMT2-null cells that can potentiate the observed mitochondrial defects. Consistent with these findings, of those enzymes which interconvert one-carbon units in the mitochondria and cytosol, only SHMT2 scored in the original genetic screen.

Restoration of one-carbon units to the mitochondria is required to rescue mitochondrial defects observed upon SHMT2 deletion

Addition of exogenous formate to cell culture media has been shown to rescue defects of one-carbon metabolism arising from combined serine starvation and glycine excess (Labuschagne et al., 2014). Formate can react with THF to generate 10-formyl THF in the cytoplasm (catalyzed by MTHFD1), and formate should be able to diffuse into the mitochondrial matrix where it can contribute to the mitochondrial one-carbon pool via an analogous reaction (catalyzed by MTHFD1L, Figure 3A). Indeed, formate addition to SHMT2-null cells was able to restore defects in mitochondrial respiration, mitochondrial encoded proteins, and proliferation in both high and low glucose (Figure 4A–D). The effect of formate addition was dose dependent, as addition of less than 500 μM formate did not restore expression of mitochondrially encoded proteins (Figure 4E, Figure S5). These data are consistent with our observation that SHMT2-null MCF10DCIS.com cells remain deficient in mitochondrially encoded proteins when grown as tumors in vivo (Figure S4M), as the circulating level of formate is approximately 33 μM (Psychogios et al., 2011).

We then asked what would be the effect of specifically preventing exogenous formate from contributing to the mitochondrial pool. We therefore deleted MTHFD1L via CRISPR/Cas9 mediated techniques in SHMT2-null Jurkat cells and verified MTHFD1L loss in single clones (Figure 4C). Jurkat cells deficient in both SHMT2 and MTHFD1L exhibited deficiencies in mitochondrial respiration, mitochondrially encoded proteins, and low glucose sensitivity, which were generally more severe than SHMT2-null cells (Figure 4C, D, F). These results further indicate that that upon SHMT2 deletion cytoplasmic formate production can only slightly compensate via MTHFD1L for loss of the mitochondrial pool. This result may be due to cytoplasmic reactions capturing the majority of THF-conjugated one carbon units and the relative inefficiency of formate import into the mitochondria and its incorporation into 10-formyl THF by MTHFD1L (Figure 3A). Indeed, the K_m of MTHFD1L for formate has been measured as 150 μM in the presence of THF-pentaglutamate (Walkup and Appling, 2005), below the ~15 μM formate concentrations observed in the cytoplasm (Lamarre et al., 2012). Importantly, treatment of cells lacking both MTHFD1L and SHMT2 with formate failed to restore mitochondrial encoded protein expression and mitochondrial respiration (Figure 4C–D). These data further demonstrate that the defects in mitochondrial metabolism observed upon SHMT2 deletion are the result of a deficiency in the mitochondrial one-carbon pool.

SHMT2-null cells are unable to maintain formylmethionyl-tRNA pools in mitochondria

We next considered whether a specific reaction occurring in the mitochondria could explain the phenotypes observed upon SHMT2 deletion. While several reactions utilize THF-conjugated cofactors, apart from the enzymes of one-carbon metabolism, only one such reaction has been demonstrated to occur in the mitochondria. The mitochondrial methionyl-tRNA formyltransferase (MTFMT) utilizes mitochondrial 10-formyl THF to produce a modified tRNA, fMet-tRNA^{Met} (Dickerman et al., 1967). This modified tRNA is specifically utilized to initiate translation in prokaryotes and in eukaryotic mitochondria, but is not required for cytoplasmic translation (Kozak, 1983). Individuals with compound heterozygous mutations in *MTFMT* exhibit Leigh syndrome and OXPHOS deficiency (Tucker et al., 2011). Fibroblasts derived from these patients exhibit an accumulation of Met-tRNA^{Met}, while in MTFMT-proficient fibroblasts the fMet-tRNA^{Met} species predominates (Tucker et al., 2011). We therefore hypothesized that cells with defects in mitochondrial one-carbon metabolism would become depleted of the 10-formyl THF cofactor and be unable to perform the MTFMT reaction, resulting in decreased mitochondrial translation and the production of proteins lacking an N-terminal formylmethionine (Figure 5A). Mitochondrially encoded tRNAs charged with formylmethionine experience a mobility shift compared to methionine-charged or uncharged tRNAs upon polyacrylamide gel electrophoresis. Moreover, fMet-tRNA^{Met} species are relatively resistant to Cu^{2+}-induced hydrolysis compared to tRNAs charged with methionine, further permitting distinction between the two tRNA species (Figure 5A). Using these methods, we observed that SHMT2-null cells exhibited substantial loss of mitochondrial fMet-tRNA^{Met} and accumulation of the non-formylated Met-tRNA^{Met} precursor, a phenotype rescued by re-expressing an SHMT2 cDNA (Figure 5B), similar to MTFMT-deficient patient fibroblasts (Tucker et al., 2011). Indeed, MTFMT-null cultured breast cancer cells exhibit a reduction in oxygen consumption, loss of mitochondrially encoded proteins, and loss of fMet-tRNA^{Met} similar to SHMT2 and MTHFD1L co-deleted cells, a phenotype slightly more severe than SHMT2 single knockout cells (Figure S6). Consistent with their effect on the levels of mitochondrially translated proteins (Figure 3H, 4C), co-deletion of SHMT2 and MTHFD1L resulted in a slightly more severe loss of fMet-tRNA^{Met} than that observed upon SHMT2 deletion, co-deletion of MTHFD2 and MTHFD2L resulted in loss of fMet-tRNA^{Met} similar to that observed upon SHMT2 deletion, and deletion of MTHFD2 alone resulted in a less severe loss of fMet-tRNA^{Met} species (Figure 5C–D). These findings are consistent with the hypothesis that mitochondrial one-carbon metabolism is required to maintain respiration through supporting production of mitochondrial formylmethionyl tRNAs.

Maintenance of mitochondrial protein levels requires minimal SHMT2 expression

Mitochondrial one-carbon metabolism is one of the most highly activated pathways in transformed tissues, leading to the hypothesis that its suppression would have anti-tumor effects (Nilsson et al., 2014; Ye et al., 2014), and reduced SHMT2 expression has been observed in aging fibroblasts concomitant with a loss of oxygen consumption, indicative of an additional role in aging tissues (Hashizume et al., 2015). We were therefore interested in asking whether physiologic fluctuations in SHMT2 expression or partial suppression, such as that which might be achievable by a small molecule inhibitor, could impact mitochondrial

function via the mechanism described above. We generated a lentivirus encoding the SHMT2 cDNA under the control of a doxycycline inducible promoter and stably infected SHMT2-null Jurkat cells (Jurkat DOXi SHMT2). When cultured in the absence of doxycycline, Jurkat DOXi SHMT2 cells expressed barely delectable levels of SHMT2, and addition of doxycycline resulted in restoration of SHMT2 protein levels (Figure 6A). However, even the minimal level of leaky SHMT2 expression exhibited in the absence of doxycycline was sufficient to maintain expression of mitochondrially encoded proteins, and additional SHMT2 expression did not further impact the expression of mitochondrially translated proteins (Figure 6A). Similarly, withdrawal of doxycycline from Jurkat DOXi SHMT2 cells previously treated with doxycycline resulted in a substantial loss of SHMT2 over 72 hours without impacting mitochondrially translated protein levels (Figure 6B). Furthermore, suppression of SHMT2 by RNAi, while leading to a substantial reduction in SHMT2 protein levels, did not impact the levels of mitochondrially translated proteins (Figure 6C). These results demonstrate that near complete loss of SHMT2 activity would be required to limit the expression of mitochondrially encoded proteins.

Discussion

Here, we describe how disruption of the mitochondrial one-carbon pool results in defects in mitochondrial respiration, the proper translation of mitochondrial proteins, and the maintenance of formylmethionyl-tRNAs utilized to initiate mitochondrial translation. Interestingly, previous experiments exploring the role of SHMT2 using RNAi mediated suppression did not observe these effects (Kim et al., 2015), consistent with our observation that low levels of SHMT2 protein are sufficient to restore translation of mitochondrial proteins. Our findings are even more surprising given results from studies using MTHFD2 knockout mouse models and analogous *S. cerevisiae* mitochondrial C(1)-tetrahydrofolate (C(1)-THF) synthase mutants, which demonstrate that MTHFD2/MIS1 deletion does not impact the translation of mitochondrial proteins (Di Pietro et al., 2002; Li et al., 2000). While the presence of MTHFD2L may rescue the effects of MTHFD2 deletion on mitochondrial translation in the mouse, *S. cerevisiae* only has one gene encoding the mitochondrial MTHFD2 homolog, MIS1. Furthermore, deletion of MIS1 results in loss of the fMet-tRNA^{Met} species in *S. cerevisiae* without impacting mitochondrial translation, leading the authors to conclude that initiation of mitochondrial translation in *S. cerevisiae* does not require Met-tRNA^{Met} formylation due to promiscuity of the mitochondrial translation initiation factor (Li et al., 2000). Therefore, species specific differences in the utilization of fMet-tRNA^{Met} to initiate mitochondrial translation may alter the effect of SHMT2 deletion across eukaryotes. The observation that MTFMT compound heterozygotes exhibit Leigh syndrome with OXPHOS deficiency is the clearest evidence that MTFMT, and by extension mitochondrial one-carbon metabolism as described here, is required for proper mitochondrial translation (Haack et al., 2014; La Piana et al., 2017; Tucker et al., 2011). A recent study of cells derived from patients with MTFMT loss-of-function have further refined the impact of its loss, arguing that the effect on translational efficiency is subunit specific, and that there may be an additional downstream effect on the stability of proteins that are translated but lack the N-terminal formylmethionine (Hinttala et al., 2015). Therefore, the observed reduction in oxygen consumption may be a compound effect on

translational efficiency, protein stability, and complex formation. However, our results do not exclude the possibility that there exist other mitochondrial reactions requiring one-carbon units to support mitochondrial translation or protein levels. Indeed, the reduction in OCR and mitochondrially encoded proteins observed upon co-deletion of MTHFD2 and MTHFD2L is similar, but not identical, to SHMT2 deletion (Figure 3H–I), while fMet-tRNA^{Met} levels are similarly affected (Figure 5D).

Eukaryotic cells maintain parallel pathways for generating THF-conjugated one-carbon units in the cytoplasm and mitochondria (Appling, 1991). Several key reactions requiring THF-conjugated one-carbon units occur in the cytoplasm or nucleus, including thymidylate synthase and phosphoribosylglycinamide formyltransferase reactions involved in nucleotide biosynthesis. Because one-carbon units for these reactions can be provided by cytoplasmic enzymes, the rationale for maintaining separate mitochondrial enzymes is unclear. Prior work has demonstrated that NADPH production by the mitochondrial pathway and the efficiency of the mitochondrial reactions in providing one carbon units for cytoplasmic reactions are important functions of this compartment (Fan et al., 2014; Ye et al., 2014). Our results are consistent with support of proper mitochondrial translation via Met-tRNA^{Met} formylation as being an additional key function of one-carbon metabolism across multiple mammalian cell types. However, maintenance of mitochondrially encoded proteins is likely to require only limited mitochondrial one-carbon pools. As such, support of N-terminal formylmethionine incorporation during mitochondrial translation is unlikely to underlie the increases in mitochondrial one-carbon metabolism observed in transformed tissues (Mejia and MacKenzie, 1985; Nilsson et al., 2014). Moreover, anti-cancer models which delete SHMT2 as a proxy for drug treatment may over-estimate the anti-cancer impact of SHMT2 perturbation, as SHMT2-deletion will inhibit mitochondrial translation, whereas the effects of drug treatment may not achieve the depletion of mitochondrial one-carbon units required to produce the same phenotype.

By identifying genes required for optimal proliferation in glucose limiting conditions, our work also provides insight into additional genes or pathways required for ETC function, and the relative impact of inhibiting individual mitochondrial complexes. Interestingly, components of Complex I scored more significantly than components of Complexes III–V in the CRISPR/Cas9 based screen reported here (Figure S1), whereas our prior work using shRNA mediated gene suppression identified members of all four complexes equally (Birsoy et al., 2014). While subtle differences in the impact of Complex I versus Complex III–V inhibition may explain this discrepancy, prior work supports the notion that cells can tolerate loss of most Complex I proteins (Stroud et al., 2016), in contrast to the core components of Complexes III, IV, and V (Birsoy et al., 2015; Wang et al., 2017). These differences in the requirement of individual subunits for cell viability could permit differential selection and scoring in genetic screens that utilize complete gene knockouts, as opposed to partial gene suppression.

Given the results presented, it is interesting to consider whether regulation of mitochondrial one carbon metabolism *in vivo* can modulate OXPHOS via impacting mitochondrial translation. Our results indicate that flux through SHMT2 plus MTHFD2/2L should be required to support mitochondrial translation *in vivo*. In contrast, flux through MTHFD1L

may only partially support the mitochondrial one carbon pool in the event that cytosolic formate levels are high, particularly given the high K_m of the enzyme for formate (Walkup and Appling, 2005), and it is not clear in what context such high concentrations would be expected. Indeed, SHMT1 knockout mice do not exhibit any overt phenotypes (MacFarlane et al., 2008), which one would expect if normal mitochondrial function was supported via cytoplasmic pools. Therefore, we would expect that tissues in which SHMT2 or MTHFD2 and MTHFD2L are expressed at very low levels might regulate mitochondrial metabolism through activation of SHMT2 or MTHFD2/2L. Based on analysis of publicly available data, SHMT2 expression is very low in the testes, breast ductal epithelium, and several central nervous system tissues, whereas MTHFD2/2L is very low in the cerebral cortex and basal ganglia. Whether expression of these genes is sufficiently low as to limit mitochondrial translation, and therefore whether activation of these enzymes in such tissues can regulate mitochondrial metabolism are unanswered questions for future work.

STAR Methods

Contact for Reagent and Resource Sharing

Further information and requests for resources and reagents should be directed to and will be fulfilled by the Lead Contact, Richard Possemato (Richard.possemato@nyumc.org). Plasmids novel to this study and corresponding sequences have been deposited at Addgene (http://www.addgene.org/).

Experimental Model and Subject Details

Cell lines—Cell lines were obtained from the following sources: Jurkat, TT, and MCF-7 from ATCC, MCF10DCIS.com cells from the Karmanos Cancer Center, Michigan, and KP murine non-small cell lung carcinoma cells from Thales Papagiannakopoulos.

Animals—Tumors were initiated into 4–8 week old female NOD.CB17 Scid/J mice orthotopically in the mouse mammary gland by implanting 500,000 MCF10DCIS.com cells in 33% matrigel into the 4^{th} murine mammary fat pad in a total volume of 25 μL. All experiments involving mice were carried out with approval from the Committee for Animal Care and under supervision of the Department of Comparative Medicine at MIT and NYU Langone Medical Center.

Method Details

Cell Culture—Cells were tested to be mycoplasma free by PCR based methods and authenticity verified by STR profiling (Duke University) for cell lines not ordered and used within one year. Cells were cultured in RPMI supplemented with 10% IFS (Sigma) and penicillin/streptomycin, except MCF10DCIS.com cells which were cultured in 50:50 DMEM and F12 media with 5% horse serum (Invitrogen) and penicillin/streptomycin.

CRISPR-Based Screen—The metabolism-focused sgRNA library of 30,000 sgRNAs (10 sgRNAs per gene) was designed and performed as previously described (Birsoy et al., 2015). Oligonucleotides for the sgRNAs were synthesized by CustomArray Inc. and amplified by PCR. Jurkat cells were infected with the sgRNA library at an MOI of 0.5, puromycin

selected for 3 days, and an initial gDNA sample was collected. Cells were grown in nutrostats (Birsoy et al., 2014) set to high (10 mM) or low (0.75 mM) glucose for 14 days, and a final gDNA sample collected. Pool deconvolution was accomplished by deep sequencing and sgRNA abundance calculated by previously described methods (Birsoy et al., 2015). We then computed the differential abundance of each sgRNA in high glucose versus low glucose and combined these sgRNA scores to arrive at a gene-level by taking the median of 10 sgRNAs targeting each gene. These values are reported in the Table S1 and in Figure 1B.

Generation of Knockout Cell Lines and cDNA Overexpression Cell Lines, and shRNA suppression—The SHMT2 open reading frame (WT or with a K280A mutation) was cloned into pMXS-IRES-Blast by direct ligation of dsDNA GeneBlocks (IDT) harboring silent mutations in the sgRNA targeting sites. sgRNAs were cloned into pLentiCRISPR, pLentiCRISPR-v2, or pSECB linearized with BsmBI with Quick ligase (New England Biolabs; M2200). These vectors along with lentiviral packaging vectors Delta-VPR and CMV VSV-G were transfected into HEK293FT cells by polyelthylenimine (Polysciences, Inc; 60 μg/mL) mediated transfection. Similarly, for overexpression cell lines, cDNA vectors along with retroviral packaging pCL-ampho were transfected into HEK293FT cells. Media was changed 24 hr after transfection and the virus-containing supernatant was collected 48 hr after transfection. Virus was passed through a 0.45 μm filter and stored at −80 °C or used immediately. Target cells in 6-well tissue culture plates were infected in media containing 2 μg/ml polybrene by spin infection at 2,250 rpm for 30 min. 24 hours post-infection, virus was removed and cells were selected with puromycin or blasticidin. For pLentiCRISPR-infected cells, after selection single cells were plated into the wells of a 96-well plate. Cells were grown for 2–3 weeks, and the resultant colonies were expanded and screened for loss of the relevant protein by immunoblotting.

For SHMT2 suppression by RNAi, lentiviral shRNAs vectors were obtained from The RNAi Consortium (TRC) collection of the Broad Institute, The TRC website is: http://portals.broadinstitute.org/gpp/public/. The TRC#s for the shRNAs used are: shLUC, TRCN0000072246; shSHMT2, TRCN0000238795. To restore SHMT2 expression upon shRNA mediated suppression, a codon optimized SHMT2 cDNA was obtained (IDT gene block) and cloned into pMXS-IRES-BLAST.

The pSECB vector was made by gibson assembly, inserting the blasticidin resistance open reading frame in place of cre recombinase from the vector pSECC (Sanchez-Rivera et al., 2014).

Immunoblotting—Cells were rinsed once in ice-cold PBS and harvested in a lysis buffer containing 50 mM Hepes, pH 7.4, 40 mM NaCl, 2 mM EDTA, 50 mM NaF, 10 mM pyrophosphate, 10 mM glycerophosphate, protease inhibitors (Roche) and 1% Triton-X-100. Protein concentrations were measured by the Bradford method or BCA Protein Assay (Pierce) and 15 μg of total lysates were resolved by SDS-PAGE (4–12% gel) and analyzed by immunoblotting as described (Minton et al., 2016).

Proliferation Assays—Direct cell counts were carried out by plating cells in triplicate in 12-well plates at 10,000 cells per well in 2 mL of media containing 1 mM or 10 mM glucose. For formate treatment, 0.5 mM sodium formate was added for three days prior to imitating proliferation assays. After 5 days, cells were counted using a Beckman Z2 Coulter Counter with a size selection setting of 8 to 30 μm.

Metabolite Profiling—5 million Jurkat cells were cultured in high or low glucose conditions for 5 days prior to metabolite extraction. Cells were rapidly washed with cold 0.8% saline, and metabolites were extracted with 80% ice-cold methanol and dried by SpeedVac. Endogenous metabolite profiles were obtained using liquid chromatography-mass spectrometry (LC-MS) as previously described (Birsoy et al., 2015). Metabolite levels (n=4 biological replicates) were normalized to protein content.

Oxygen Consumption Measurements—Oxygen consumption of cells was measured using an XFe24 Extracellular Flux Analyzer (Seahorse Bioscience). For suspension cells, seahorse plates were coated with Cell-TAK (Corning; 0.02 mg/mL in 0.1 μM $NaHO_3$) for 20 min. Then 200,000 cells were attached to the plate by centrifugation at 1,000*g*, without brakes for 5 min. For adherent cells, 30,000 to 80,000 cells were plated the night before the experiment. RPMI was used as the assay media for all experiments with 1 mM glucose (low glucose) or 10 mM glucose (high glucose) in the presence of 2 mM glutamine without serum. For basal oxygen consumption measurements, cell number was used for normalization.

Mitochondrial DNA copy number, mass, membrane potential, and expression —For copy number, total DNA was isolated and qPCR was performed. *Alu* repeat elements were used as controls. Primers used were: *ND1* forward and reverse, CCCTAAAACCCGCCACATCT and GAGCGATGGTGAGAGCTAAGGT; *ND2* forward and reverse, TGTTGGTTATACCCTTCCCGTACTA and CCTGCAAAGATGGTAGAGTAGATGA; *Alu* forward and reverse, CTTGCAGTGAGCCGAGATT and GAGACGGAGTCTCGCTCTGTC.

For mitochondrial mass measurements, 1×10^6 cells were incubated with 75 nM Mitotracker Green FM (Invitrogen; M7514) in RPMI for 1 hr at 37 °C. Cells were then centrifuged at 1,000*g* for 5 min at 4 °C and the overlying media removed. Cells were kept on ice, washed once with PBS, and resuspended in fresh PBS for flow cytometry analysis of live cells. The mean Mitotracker Green fluorescence intensity was used as a measure of relative mitochondrial mass.

For mitochondrial membrane potential, 1×10^5 cells were incubated with 200 nM tetramethylrhodamine, methyl ester, perchlorate (TMRE) stain (Life Technologies; T668) in RPMI for 20 min at 37 °C, washed once with PBS, and resuspended in fresh PBS for flow cytometry analysis of live cells. For FCCP treatment, cells were incubated with 20 μM FCCP for 10 min prior to adding TMRE stain. The mean TRME fluorescence intensity was used as a measure of relative mitochondrial membrane potential.

The following primers were used to analyze the expression of mitochondrially encoded genes by qPCR are provided in Table S2.

Mitochondrial and Cytoplasmic Translation Assay—Mitochondrial or cytoplasmic protein translation was assessed by labeling with ^{35}S-methionine/^{35}S-cysteine (EXPRE35S35S Protein Labeling Mix; Perkin Elmer Life Sciences). 5×10^6 cells were incubated in RPMI media lacking methionine for 6 hours prior to cycloheximide (Sigma, C7698) treatment or 30 minutes prior to emetine (Millipore, 324693) and chloramphenicol (Sigma, C0378) treatment. The inhibitors (100 μg/ml) were added and cells were incubated for 15 minutes. 55 μCi ^{35}S-methionine/^{35}S-cysteine was then added to media and cells were incubated at 37 °C for an additional 2 hours (cycloheximide treated samples) or 1 hour (chloramphenicol and emetine treated samples). Cells were washed with ice-cold PBS and RIPA lysis buffer was added. Mitochondrial proteins (60 μg) were analyzed by SDS-PAGE using 16% tris-glycine gel in tris-glycine running buffer, and cytoplasmic proteins (20 μg) using 4–12% bis-tris gel in MES running buffer. Total protein levels were assessed by coomassie blue staining (0.1% coomassie blue in 7% acetic acid and 40% methanol), and ^{35}S labeled proteins were assayed by autoradiography using BioMax MR film (Sigma, Z350370) or phosphor imaging screen (Bio-Rad, 170-7841).

Northern blot analysis of mitochondrial Mef/fMet-tRNA^{Met}—Analysis of mitochondrial tRNAs was performed essentially as described in (Kohrer and Rajbhandary, 2008) with the following details and modifications: 2.5×10^7 cells were lysed in TRIzol (Life Technologies, 15596026) and total RNA was extracted according to the manufacturer's instructions except that RNA pellet was washed using 75% ethanol containing 10 mM sodium acetate (pH 4.9). Aqueous phase of each sample was divided into 3 parts. After isopropanol precipitation and ethanol wash, each RNA pellet was subject to the following treatments. The first sample was resuspended in 10 mM sodium acetate (pH 4.9) and incubated at 37 °C for 30 minutes (control treatment). The second sample was resuspended in 200 mM sodium acetate (pH 4.9) containing 10 mM $CuSO_4$ and incubated at 37 °C for 30 minutes to selectively deacylate Met-tRNA^{Met} (Guillon et al., 1992). The reaction was terminated by adding 10 mM EDTA. The third sample was resuspended in 100 mM Tris-Cl (pH 9.6) and incubated at 65 °C for 5 minutes, followed by incubation at 37 °C for 1 hr. This treatment deacylates all amino acid-charged tRNAs (Kohrer and Rajbhandary, 2008). Following treatment, the samples were ethanol-precipitated and redissolved in 10 mM sodium acetate (pH 4.9). The RNA concentration was measured by a Nanodrop spectrophotometer. Acid-urea PAGE and northern blotting were then performed as previously described with slight modifications (Kohrer and Rajbhandary, 2008; Nilsson et al., 2014). Brifely, 5–7 μg of total RNA was separated on an 8.5% acid-urea polyacylamide gel (17.1W × 32.5H cm, 0.4 mm thick) using a sequencing gel apparatus (Model SA, Gibco-BRL). After running at 500 volts for 14–18 hours, RNAs were transferred onto positively charged nylon membrane (Hybond-N$^+$ #RPN303B, GE Healthcare). The membrane was baked at 70 °C for 1.5 hours and then prehybridized at 42 °C for 6 hours. The probe specific for mitochondrial tRNA^{Met} (5′-TAGTACGGGAAGGGTATAA-3′) was labeled at 5′-end with ^{32}P-γ-ATP (PerkinElmer) using T4 polynucleotide kinase (NEB). The membrane was hybridized with the labeled probe at 42 °C for 20–24 hours, followed by two washes with 6x

SSC and one wash with 4x SSC at room temperature (each wash for 10 minutes). The membrane was then exposed to a BioMax MR film (Kodak) to visualize bands at −80 °C for 1–3 days.

Quantification and Statistical Analysis

Experiments were repeated at least three times with the following exceptions, the CRISPR screen (Fig. 1A–B, S1), which was performed once. P-values reported in the figures are the result of heteroscedastic Student's t-tests and distributions assumed to follow a Student's t distribution. These assumptions are not contradicted by the data. No samples or animals were excluded from analysis and sample size estimates were not used. The number of independent biological replicates (n) are indicated in the figure legend and represent replicate measurements from distinct samples. For immunoblots and autoradiograpy, the reported images are representative of at least three independent experiments. Studies were not conducted blind.

Data and Software Availability

Primary data from this manuscript has been uploaded to Mendeley Data and can be accessed at http://dx.doi.org/10.17632/pb2yh64pcj.1

Supplementary Material

Refer to Web version on PubMed Central for supplementary material.

Acknowledgments

We thank all members of the Birsoy and Possemato labs for helpful suggestions. pLENTICRISPR was a kind gift of F. Zhang. This research is supported by the NIH (T32GM007308 supporting V.O.S., T32CA009161 supporting D.J.M., K22CA193660 to K.B., and R00CA168940 to R.P.), the Jimmy V Foundation (R.P.), Susan G. Komen for the Cure (R.P.), the Irma-Hirschl Trust (K.B.), and an AACR NextGen Grant (K.B.). D.M.S. is an investigator of the Howard Hughes Medical Institute. R.P is a Pew-Stewart Scholar. K.B. is a Searle Scholar, Sidney Kimmel Scholar and Basil O'Connor Scholar of the March of Dimes. The Experimental Pathology Resource Center is partially supported by the Cancer Center Support Grant, P30CA016087, at the Laura and Isaac Perlmutter Cancer Center, and the NIH (S10 OD010584-01A1 and S10 OD018338-01). The Immune Monitoring Core is supported by the NIH (S10 OD016304-01).

References

Appling DR. Compartmentation of folate-mediated one-carbon metabolism in eukaryotes. Faseb J. 1991; 5:2645–2651. [PubMed: 1916088]

Arroyo JD, Jourdain AA, Calvo SE, Ballarano CA, Doench JG, Root DE, Mootha VK. A Genome-wide CRISPR Death Screen Identifies Genes Essential for Oxidative Phosphorylation. Cell metabolism. 2016; 24:875–885. [PubMed: 27667664]

Birsoy K, Possemato R, Lorbeer FK, Bayraktar EC, Thiru P, Yucel B, Wang T, Chen WW, Clish CB, Sabatini DM. Metabolic determinants of cancer cell sensitivity to glucose limitation and biguanides. Nature. 2014; 508:108–112. [PubMed: 24670634]

Birsoy K, Wang T, Chen WW, Freinkman E, Abu-Remaileh M, Sabatini DM. An Essential Role of the Mitochondrial Electron Transport Chain in Cell Proliferation Is to Enable Aspartate Synthesis. Cell. 2015; 162:540–551. [PubMed: 26232224]

Calvo SE, Clauser KR, Mootha VK. MitoCarta2.0: an updated inventory of mammalian mitochondrial proteins. Nucleic acids research. 2016; 44:D1251–1257. [PubMed: 26450961]

Cantor JR, Sabatini DM. Cancer cell metabolism: one hallmark, many faces. Cancer discovery. 2012; 2:881–898. [PubMed: 23009760]

Crabtree HG. Observations on the carbohydrate metabolism of tumours. The Biochemical journal. 1929; 23:536–545. [PubMed: 16744238]

Di Pietro E, Sirois J, Tremblay ML, MacKenzie RE. Mitochondrial NAD-dependent methylenetetrahydrofolate dehydrogenase-methenyltetrahydrofolate cyclohydrolase is essential for embryonic development. Mol Cell Biol. 2002; 22:4158–4166. [PubMed: 12024029]

Dickerman HW, Steers E Jr, Redfield BG, Weissbach H. Methionyl soluble ribonucleic acid transformylase. I. Purification and partial characterization. The Journal of biological chemistry. 1967; 242:1522–1525. [PubMed: 5337045]

Ducker GS, Rabinowitz JD. One-Carbon Metabolism in Health and Disease. Cell metabolism. 2017; 25:27–42. [PubMed: 27641100]

Fan J, Ye J, Kamphorst JJ, Shlomi T, Thompson CB, Rabinowitz JD. Quantitative flux analysis reveals folate-dependent NADPH production. Nature. 2014; 510:298–302. [PubMed: 24805240]

Guillon JM, Mechulam Y, Schmitter JM, Blanquet S, Fayat G. Disruption of the gene for Met-tRNA(fMet) formyltransferase severely impairs growth of Escherichia coli. Journal of bacteriology. 1992; 174:4294–4301. [PubMed: 1624424]

Gullino PM, Grantham FH, Courtney AH. Glucose consumption by transplanted tumors in vivo. Cancer research. 1967; 27:1031–1040. [PubMed: 4290857]

Haack TB, Gorza M, Danhauser K, Mayr JA, Haberberger B, Wieland T, Kremer L, Strecker V, Graf E, Memari Y, et al. Phenotypic spectrum of eleven patients and five novel MTFMT mutations identified by exome sequencing and candidate gene screening. Molecular genetics and metabolism. 2014; 111:342–352. [PubMed: 24461907]

Hashizume O, Ohnishi S, Mito T, Shimizu A, Ishikawa K, Nakada K, Soda M, Mano H, Togayachi S, Miyoshi H, et al. Epigenetic regulation of the nuclear-coded GCAT and SHMT2 genes confers human age-associated mitochondrial respiration defects. Sci Rep. 2015; 5:10434. [PubMed: 26000717]

Hinttala R, Sasarman F, Nishimura T, Antonicka H, Brunel-Guitton C, Schwartzentruber J, Fahiminiya S, Majewski J, Faubert D, Ostergaard E, et al. An N-terminal formyl methionine on COX 1 is required for the assembly of cytochrome c oxidase. Hum Mol Genet. 2015; 24:4103–4113. [PubMed: 25911677]

Hirayama A, Kami K, Sugimoto M, Sugawara M, Toki N, Onozuka H, Kinoshita T, Saito N, Ochiai A, Tomita M, et al. Quantitative metabolome profiling of colon and stomach cancer microenvironment by capillary electrophoresis time-of-flight mass spectrometry. Cancer research. 2009; 69:4918–4925. [PubMed: 19458066]

Kim D, Fiske BP, Birsoy K, Freinkman E, Kami K, Possemato RL, Chudnovsky Y, Pacold ME, Chen WW, Cantor JR, et al. SHMT2 drives glioma cell survival in ischaemia but imposes a dependence on glycine clearance. Nature. 2015; 520:363–367. [PubMed: 25855294]

Kohrer C, Rajbhandary UL. The many applications of acid urea polyacrylamide gel electrophoresis to studies of tRNAs and aminoacyl-tRNA synthetases. Methods. 2008; 44:129–138. [PubMed: 18241794]

Kozak M. Comparison of initiation of protein synthesis in procaryotes, eucaryotes, and organelles. Microbiological reviews. 1983; 47:1–45. [PubMed: 6343825]

La Piana R, Weraarpachai W, Ospina LH, Tetreault M, Majewski J, Bruce Pike G, Decarie JC, Tampieri D, Brais B, et al. Care4Rare Canada C. Identification and functional characterization of a novel MTFMT mutation associated with selective vulnerability of the visual pathway and a mild neurological phenotype. Neurogenetics. 2017; 18:97–103. [PubMed: 28058511]

Labuschagne CF, van den Broek NJ, Mackay GM, Vousden KH, Maddocks OD. Serine, but not glycine, supports one-carbon metabolism and proliferation of cancer cells. Cell reports. 2014; 7:1248–1258. [PubMed: 24813884]

Lamarre SG, Molloy AM, Reinke SN, Sykes BD, Brosnan ME, Brosnan JT. Formate can differentiate between hyperhomocysteinemia due to impaired remethylation and impaired transsulfuration. American journal of physiology Endocrinology and metabolism. 2012; 302:E61–67. [PubMed: 21934042]

Li Y, Holmes WB, Appling DR, RajBhandary UL. Initiation of protein synthesis in Saccharomyces cerevisiae mitochondria without formylation of the initiator tRNA. Journal of bacteriology. 2000; 182:2886–2892. [PubMed: 10781559]

MacFarlane AJ, Liu X, Perry CA, Flodby P, Allen RH, Stabler SP, Stover PJ. Cytoplasmic serine hydroxymethyltransferase regulates the metabolic partitioning of methylenetetrahydrofolate but is not essential in mice. The Journal of biological chemistry. 2008; 283:25846–25853. [PubMed: 18644786]

Mejia NR, MacKenzie RE. NAD-dependent methylenetetrahydrofolate dehydrogenase is expressed by immortal cells. The Journal of biological chemistry. 1985; 260:14616–14620. [PubMed: 3877056]

Minton DR, Fu L, Mongan NP, Shevchuk MM, Nanus DM, Gudas LJ. Role of NADH Dehydrogenase (Ubiquinone) 1 Alpha Subcomplex 4-Like 2 in Clear Cell Renal Cell Carcinoma. Clinical cancer research: an official journal of the American Association for Cancer Research. 2016; 22:2791–2801. [PubMed: 26783287]

Momb J, Lewandowski JP, Bryant JD, Fitch R, Surman DR, Vokes SA, Appling DR. Deletion of Mthfd1l causes embryonic lethality and neural tube and craniofacial defects in mice. Proceedings of the National Academy of Sciences of the United States of America. 2013; 110:549–554. [PubMed: 23267094]

Nilsson R, Jain M, Madhusudhan N, Sheppard NG, Strittmatter L, Kampf C, Huang J, Asplund A, Mootha VK. Metabolic enzyme expression highlights a key role for MTHFD2 and the mitochondrial folate pathway in cancer. Nature communications. 2014; 5:3128.

Psychogios N, Hau DD, Peng J, Guo AC, Mandal R, Bouatra S, Sinelnikov I, Krishnamurthy R, Eisner R, Gautam B, et al. The human serum metabolome. PloS one. 2011; 6:e16957. [PubMed: 21359215]

Robinson BH, Petrova-Benedict R, Buncic JR, Wallace DC. Nonviability of cells with oxidative defects in galactose medium: a screening test for affected patient fibroblasts. Biochemical medicine and metabolic biology. 1992; 48:122–126. [PubMed: 1329873]

Sanchez-Rivera FJ, Papagiannakopoulos T, Romero R, Tammela T, Bauer MR, Bhutkar A, Joshi NS, Subbaraj L, Bronson RT, Xue W, et al. Rapid modelling of cooperating genetic events in cancer through somatic genome editing. Nature. 2014; 516:428–431. [PubMed: 25337879]

Schirch D, Delle Fratte S, Iurescia S, Angelaccio S, Contestabile R, Bossa F, Schirch V. Function of the active-site lysine in Escherichia coli serine hydroxymethyltransferase. The Journal of biological chemistry. 1993; 268:23132–23138. [PubMed: 8226831]

Stover P, Schirch V. Serine Hydroxymethyltransferase Catalyzes the Hydrolysis of 5,10-Methenyltetrahydrofolate to 5-Formyltetrahydrofolate. Journal of Biological Chemistry. 1990; 265:14227–14233. [PubMed: 2201683]

Stroud DA, Surgenor EE, Formosa LE, Reljic B, Frazier AE, Dibley MG, Osellame LD, Stait T, Beilharz TH, Thorburn DR, et al. Accessory subunits are integral for assembly and function of human mitochondrial complex I. Nature. 2016; 538:123–126. [PubMed: 27626371]

Sullivan LB, Gui DY, Hosios AM, Bush LN, Freinkman E, Vander Heiden MG. Supporting Aspartate Biosynthesis Is an Essential Function of Respiration in Proliferating Cells. Cell. 2015; 162:552–563. [PubMed: 26232225]

Tucker EJ, Hershman SG, Kohrer C, Belcher-Timme CA, Patel J, Goldberger OA, Christodoulou J, Silberstein JM, McKenzie M, Ryan MT, et al. Mutations in MTFMT underlie a human disorder of formylation causing impaired mitochondrial translation. Cell metabolism. 2011; 14:428–434. [PubMed: 21907147]

Vander Heiden MG, DeBerardinis RJ. Understanding the Intersections between Metabolism and Cancer Biology. Cell. 2017; 168:657–669. [PubMed: 28187287]

Walkup AS, Appling DR. Enzymatic characterization of human mitochondrial C1-tetrahydrofolate synthase. Arch Biochem Biophys. 2005; 442:196–205. [PubMed: 16171773]

Wallace DC. Mitochondrial diseases in man and mouse. Science. 1999; 283:1482–1488. [PubMed: 10066162]

Wang T, Yu H, Hughes NW, Liu B, Kendirli A, Klein K, Chen WW, Lander ES, Sabatini DM. Gene Essentiality Profiling Reveals Gene Networks and Synthetic Lethal Interactions with Oncogenic Ras. Cell. 2017; 168:890–903. e815. [PubMed: 28162770]

Ye J, Fan J, Venneti S, Wan YW, Pawel BR, Zhang J, Finley LW, Lu C, Lindsten T, Cross JR, et al. Serine catabolism regulates mitochondrial redox control during hypoxia. Cancer discovery. 2014; 4:1406–1417. [PubMed: 25186948]

Highlights

- Cells lacking SHMT2 are sensitive to glucose restriction
- The mitochondrial one-carbon pool supports respiration
- SHMT2 loss disrupts proper translation of mitochondrially encoded proteins
- Serine contributes to methionine formylation on mitochondrial initiator tRNAs

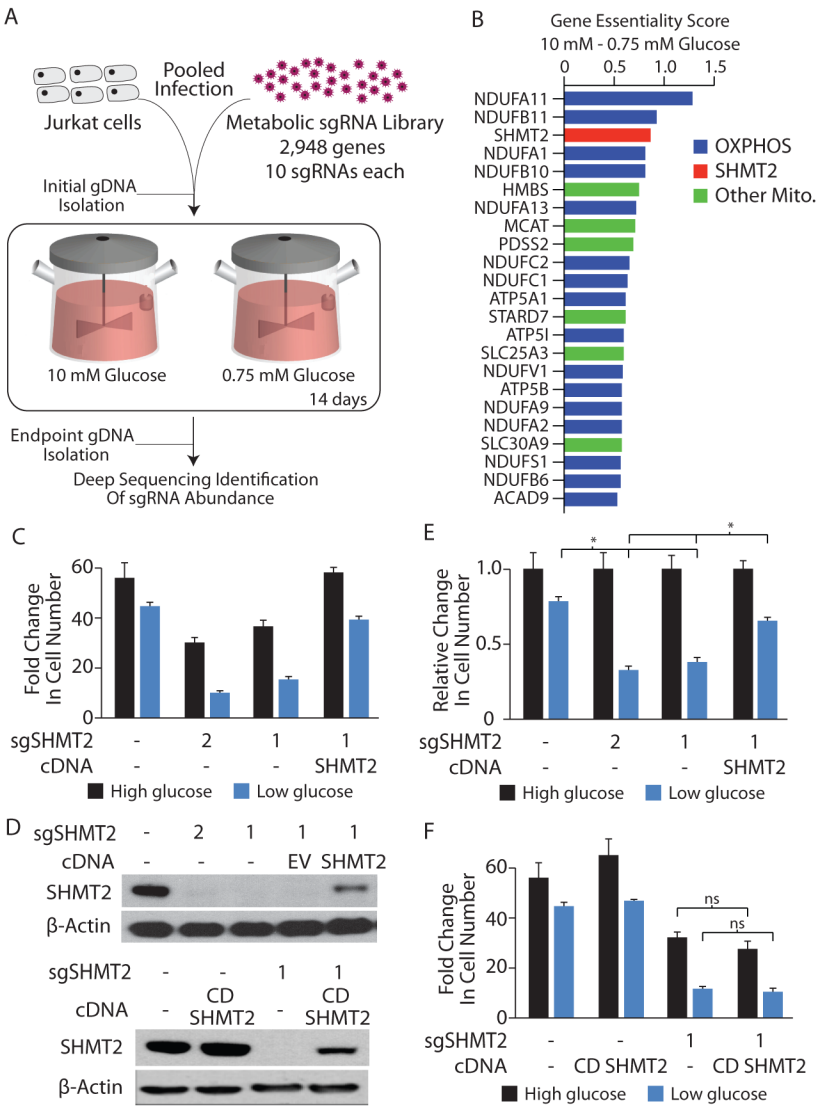

Figure 1. A CRISPR/Cas9 based genetic screen identifies SHMT2 as being differentially required in low glucose conditions

A, Pooled screening outline. An sgRNA library targeting 2,948 metabolic enzymes and small molecule transporters was transduced into Jurkat T cells followed by culture in Nutrostats set to 10 mM or 0.75 mM glucose for a period of 14 days. Genomic DNA was collected prior to or after the 14 day period and the abundance of sgRNAs determined by deep sequencing. B, Genes exhibiting differential essentiality in 0.75 mM glucose, compared to 10 mM glucose, median Log_2 fold change cutoff of 0.5. Genes indicated in blue are components of oxidative phosphorylation complexes, while those in green are also mitochondrially localized. C, Proliferation of Jurkat cells or clones expressing small guide RNAs targeting SHMT2 (sgSHMT2), or with reintroduction of the SHMT2 cDNA. Cells were grown for 5 days in media initially containing 10 mM (high glucose) or 1.5 mM glucose (low glucose). D, Immunoblot for SHMT2 or beta-actin from cell lysates of the lines described in *C* (above), or expressing a catalytically inactive mutant (K280A) of SHMT2 (CD SHMT2) (below). E, Data from *C*, normalized to the 10 mM glucose condition for each

cell line. F, Proliferation as in *C*, using the cell lines indicated. * $p < 0.05$, ns = not significant. Error bars are s.e.m. n=3 for cell proliferation experiments.

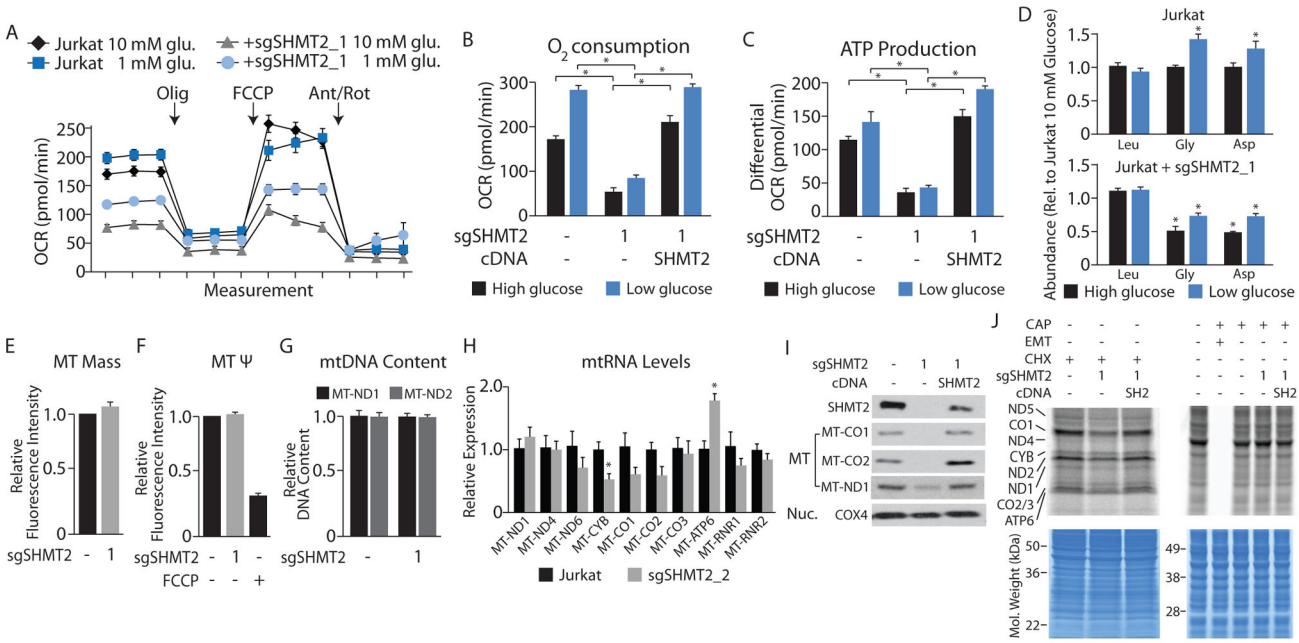

Figure 2. SHMT2 is required for proper mitochondrial respiration and translation of mitochondrially encoded proteins

A, Oxygen consumption rate (OCR) of Jurkat cells cultured at the indicated glucose concentrations from a representative experiment. Jurkat cells or a clone expressing small guide RNAs targeting SHMT2 (sgSHMT2) were seeded at 200,000 cells per well immediately prior to the assay. The complex V inhibitor oligomycin (Olig), the uncoupler carbonyl cyanide 4-(trifluoromethoxy)phenylhydrazone (FCCP), and the complex I and III inhibitors Antimycin (Ant) and Rotenone (Rot) were added sequentially to a final concentration of 1 μM at the indicated time points. B, Basal OCR from the lines described in *A* and cells re-expressing an SHMT2 cDNA. C, Proportion of OCR contributing to ATP production (measured as the decrease in OCR upon oligomycin treatment) from the lines described in *A–B*. D, Intracellular levels of the indicated amino acids in the indicated cell lines cultured in media containing 10 mM (high glucose) or 1.5 mM glucose (low glucose), as measured by LC/MS. E, Relative mitochondrial mass as assessed by flow cytometry based measurement of fluorescence from the indicated Jurkat cell lines stained with mitotracker green FM (75 nM). F, Relative mitochondrial membrane potential (Ψ) as assessed by flow cytometry based measurement of fluorescence from the indicated Jurkat cell lines stained with tetramethylrhodamine, methyl ester, perchlorate (200 nM). Indicated cells were treated with FCCP (20 μM). G, Relative mitochondrial DNA content in Jurkat cell lines as assessed by qPCR based measurement of the indicated mtDNA genes, normalized to an *Alu* repeat sequence. H, Relative mitochondrial expression in Jurkat cell lines as assessed by qPCR based measurement of the indicated mitochondrial genes. I, Immunoblot from cell lysates of the indicated lines for proteins encoded by the indicated genes. MT-CO1, MT-CO2, and MT-ND1 are encoded by the mitochondrial genome and translated in the mitochondria (MT) whereas COX4 is encoded by the nuclear genome and translated in the cytoplasm (Nuc.). J, ^{35}S-cysteine and ^{35}S-methionine pulsed labeling of mitochondrial proteins (top left, 60 μg) or cytoplasmic proteins of a similar size (top right, 20 μg) from the

indicated cell lines. Compounds used to inhibit translation are chloramphenicol (CAP, 100 μg/mL), emetine (EM, 100 μg/mL), or cycloheximide (CHX, 100 μg/mL). Gels stained for total protein with coomassie blue as a loading control, molecular weight markers indicated (bottom). The identity of individual mitochondrial proteins is indicated on the right and is inferred by comparing the banding pattern to published results (Tucker et al., 2011) as well as subsequent immunoblotting for CO1 and CO2. * $p < 0.05$. Error bars are s.e.m. n=4–5 for *A*, n=3 for *B–H*.

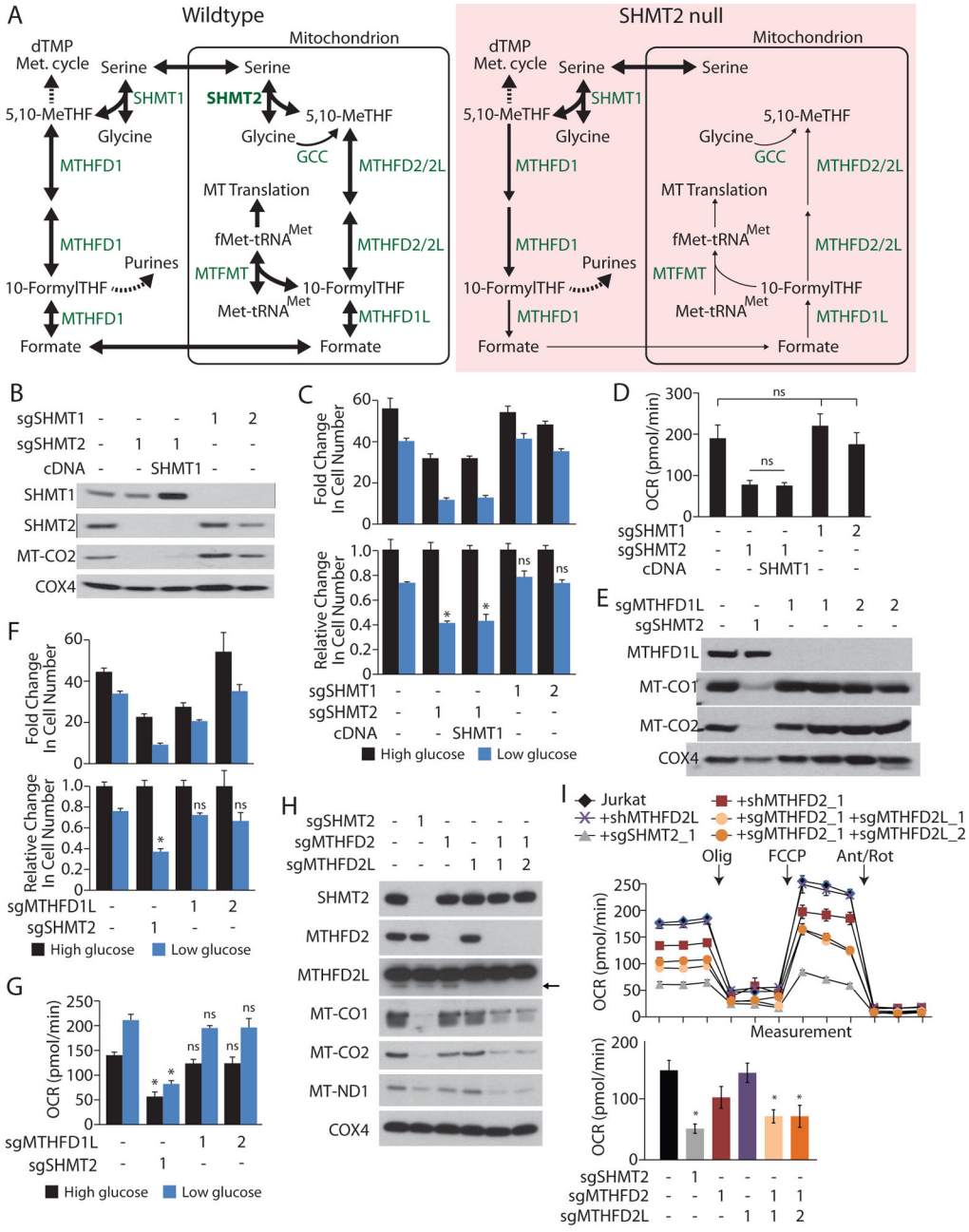

Figure 3. Depletion of mitochondrial one-carbon units upon SHMT2 loss prevents proper mitochondrial translation

A, Overview schematic of one-carbon metabolism indicating cytoplasmic and mitochondrial compartmentalization in wildtype cells (left), and proposed alterations upon SHMT2 deletion (right). While reactions are reversible, arrow direction and thickness indicate hypothetical relative flux upon SHMT2 deletion. Enzymes and the glycine cleavage complex (GCC) are indicated in green. Key metabolites are indicated in black. THF = tetrahydrofolate. B, E, and H, Immunoblot from cell lysates of Jurkat cell lines for proteins encoded by the indicated genes. Jurkat cell clones express sgRNAs targeting SHMT1, SHMT2, MTHFD1L, MTHFD2, or MTHFD2L or a cDNA expressing SHMT1, as

indicated. For the MTHFD2L immunoblot in panel H, the arrow indicates the band corresponding to MTHFD2L protein, whereas the prominent larger band is non-specific. C and F, Above, proliferation of Jurkat cells or clones expressing the indicated sgRNAs and cDNAs. Below, data from above, normalized to the 10 mM glucose condition for each cell line. Cells were grown for 5 days in media initially containing 10 mM (high glucose) or 1.5 mM glucose (low glucose). D, Basal oxygen consumption rate (OCR) of the cell lines from *A*, cultured in 10 mM glucose. G, Basal oxygen consumption rate (OCR) of the cell lines from *F*, cultured in 10 mM (high glucose) or 1.5 mM glucose (low glucose). I, Basal oxygen consumption rate (OCR) of the cell lines from *H*, cultured in 10 mM glucose. * $p < 0.05$, ns = not significant. Unless otherwise indicated, these statistical measurements are in reference to Jurkat cells cultured at the same glucose concentration. Error bars are s.e.m. n=3 for *C, D, G, I*; n=6 for *F*.

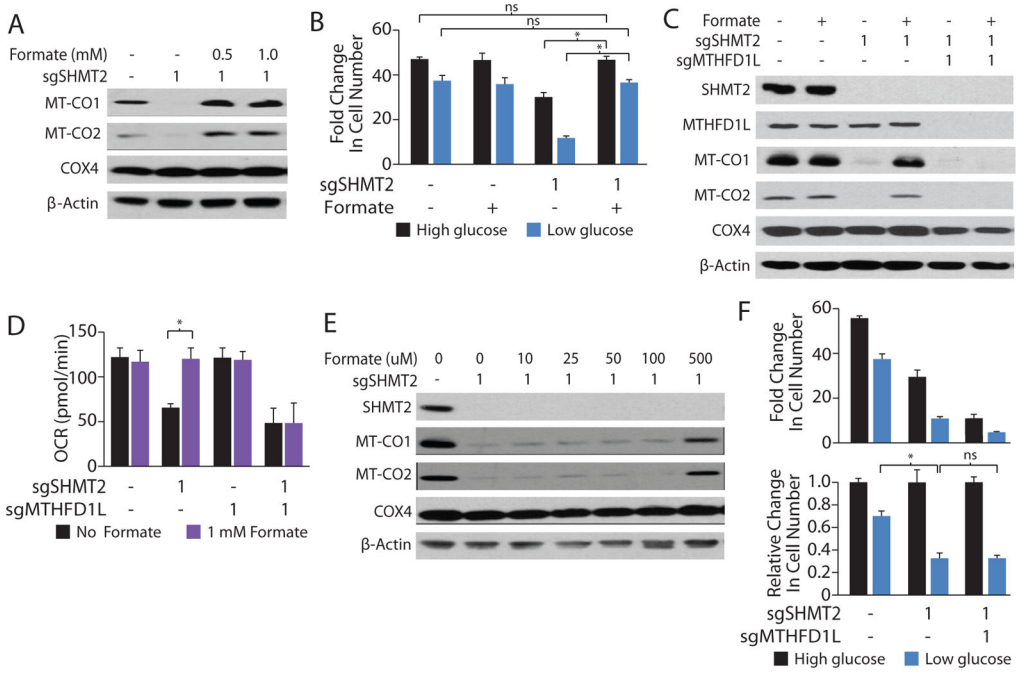

Figure 4. Restoration of one-carbon units to the mitochondria is required to rescue mitochondrial defects observed upon SHMT2 deletion

A, C, E, Immunoblot from cell lysates of Jurkat cell lines for proteins encoded by the indicated genes, upon addition of the indicated concentration of sodium formate for 3 days. B, Proliferation of Jurkat cells or clones from *A*, treated with the indicated concentration of sodium formate for 3 days prior to measurement. Cells were then grown for 5 days in media initially containing 10 mM (high glucose) or 1.5 mM glucose (low glucose). D, Basal oxygen consumption rate (OCR) of the cell lines from *C*, cultured in 10 mM glucose and the indicated concentration of sodium formate for 3 days. F, Above, proliferation of Jurkat cells or clones expressing the indicated sgRNAs and cDNAs. Below, data from above, normalized to the 10 mM glucose condition for each cell line. Cells were grown for 5 days in media initially containing 10 mM (high glucose) or 1.5 mM glucose (low glucose). * $p < 0.05$, ns = not significant. Error bars are s.e.m. n=3.

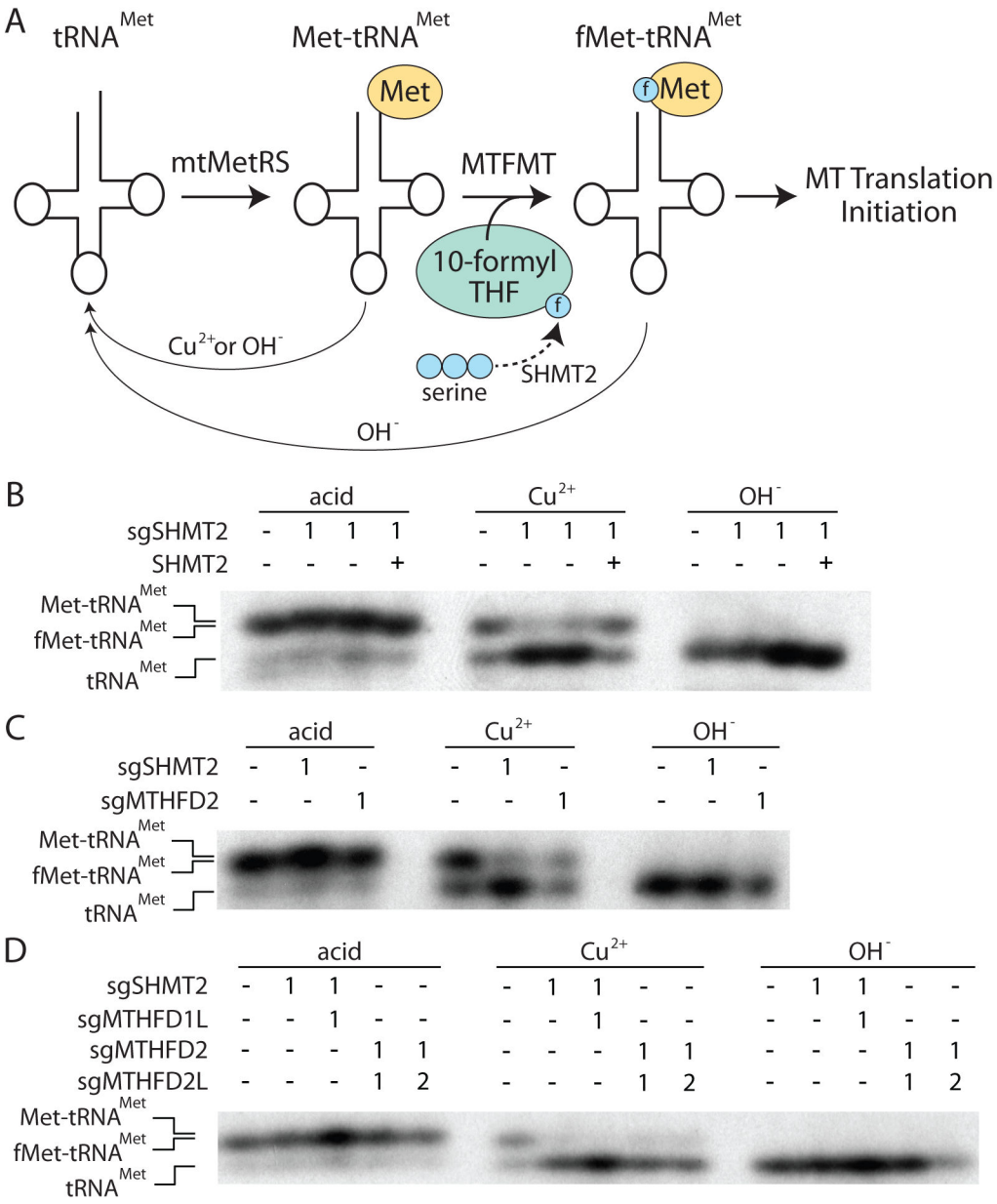

Figure 5. SHMT2-null cells are unable to maintain formylmethionyl-tRNA pools in mitochondria

A, Schematic overview of mitochondrial $tRNA^{Met}$ maturation and sensitivity to Cu^{2+} or OH^- treatment. Uncharged $tRNA^{Met}$ is charged by the mitochondrial methionyl tRNA synthetase (mtMetRS) to form $Met\text{-}tRNA^{Met}$. This species is further modified by MTFMT using a formyl group (blue circle marked with an "f"), derived from serine via the SHMT2 reaction, forming $fMet\text{-}tRNA^{Met}$. The $fMet\text{-}tRNA^{Met}$ is then used to initiate translation in the mitochondria. Upon treatment with Cu^{2+} or OH^-, $Met\text{-}tRNA^{Met}$ is hydrolyzed to $tRNA^{Met}$, whereas $fMet\text{-}tRNA^{Met}$ is relatively resistant to Cu^{2+} treatment. B–D, Detection of mitochondrial $tRNA^{Met}$ species by northern blot using a probe specific to the mitochondrial $tRNA^{Met}$ and RNA isolated from Jurkat cell clones expressing an sgRNA targeting SHMT2 or additionally re-expressing SHMT2, or clones expressing an sgRNA

targeting MTHFD1L, MTHFD2, or MTHFD2L. Met and fMet modification of the tRNA alters its mobility as indicated on the left. RNA was isolated under acidic conditions to preserve fMet or Met charged species (left) or treated to selectively hydrolyze Met (Cu^{2+}, middle) or non-selectively hydrolyze both fMet and Met (OH^{-}, right).

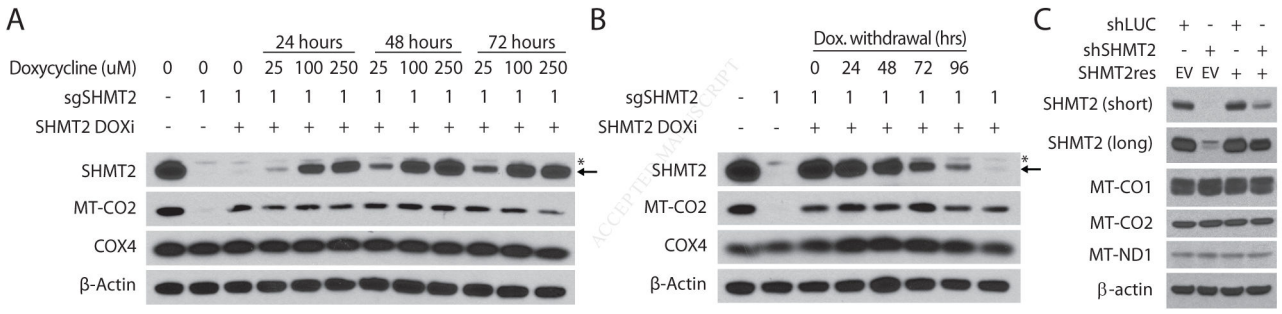

Figure 6. Maintenance of mitochondrial protein levels requires minimal SHMT2 expression

A, Immunoblot from cell lysates of Jurkat cells or SHMT2-null Jurkat cell lines clones expressing an SHMT2 cDNA under the control of a doxycycline-inducible promoter (DOXi SHMT2), for proteins encoded by the indicated genes. Doxycycline was added at the indicated concentrations for the indicated number of days. For the SHMT2 immunoblot, the arrow indicates the band corresponding to SHMT2 protein, whereas the larger band (*) is non-specific and visible at the exposure shown. B, Immunoblot as in *A*. Doxycycline was added at the indicated concentration for 3 days and then withdrawn for the indicated number of days. C, Immunoblots from cell lysates of Jurkat cells expressing shRNAs targeting SHMT2 with or without expression of a codon-optimized, shRNA-resistant SHMT2 cDNA (SHMT2res).